Chiral Quadridentate Ligands Derived from Amino Acids and Some Zinc Complexes Thereof

Nicole Niklas,[a] Olaf Walter,[b] and Ralf Alsfasser*[a]

Dedicated to Prof. Dr. Heinrich Vahrenkamp on the occasion of his 60th birthday

Keywords: Bioinorganic chemistry / Zinc / Amino acids / Chiral ligands / Tripodal ligands

A series of three new quadridentate ligands was synthesized by reaction of the haloacetylated amino acid esters L-BrAc–Phe–OMe (**4a**), L-BrAc–Lys(Z)–OMe (**4b**), and ClAc–Gly–OEt (**4c**), respectively, with bis(picolyl)amine (bpa, **5**). The obtained products L-bpaAc–Phe–OMe (**3a**), L-bpaAc–Lys(Z)–OMe (**3b**), and bpaAc–Gly–OEt (**3c**) were treated with $Zn(OTf)_2$ (OTf = $CF_3SO_3^-$) to yield the trigonal-bipyramidal complexes [(L-bpaAc–Phe–OMe)ZnOTf](OTf) (**6a**), [(L-bpaAc–Lys(Z)–OMe)ZnOTf](OTf) (**6b**), and [(bpaAc–Gly–OEt)ZnOTf](OTf) (**6c**). Crystal structures of **6c** and the hydrolysis product [(L-bpaAc–Phe–OMe)-(H_2O)ZnOTf]$(OTf)_2$ (**7a**) are reported. The results suggest the formation of a chiral pocket at the metal center provided by the benzyl substituent in the L-phenylalanine derivative **7a**. This observation is further supported by ^{1}H-NMR and circular dichroism spectroscopic data. These methods indicate a significant ordering effect within the ligands upon metal coordination as well as interactions between the first coordination spheres and their chiral environments provided by the L-phenylalanine and L-lysine moieties of **3a** and **3b**, respectively. Our results are discussed with respect to the development of chiral building blocks for transition metal catalysts and biomimetic assemblies.

Introduction

Apart from their importance in biological systems, amino acids are versatile building blocks for a variety of fascinating synthetic molecular and supramolecular assemblies such as peptide nucleic acids (PNAs),[1] dendrimers,[2] micelles,[3] or de novo designed peptides[4] and proteins.[5,6] The scope of accessible amino acid side-chain functionalities has been tremendously broadened by organic chemists who have developed different methods for the enantioselective synthesis and processing of artificial amino acids carrying, for example, aromatic rings,[7] sugars,[8] or organic cofactors such as pyridoxamine[9] and flavine.[10] The latter two examples illustrate the potential of nonnatural amino acids as catalytically active components for the design of new materials.

Catalytically active amino acid derivatives are attractive targets not only for organic chemists but also for coordination chemistry. There is a still growing interest in metal complexes as enantioselective catalysts for organic conversions such as oxidations,[11,12] carbon−carbon bond formations,[13] or hydrolytic cleavage reactions.[14,15] Metal complexes of synthetic amino acids with covalently attached synthetic polydentate chelators are interesting building blocks for polyfunctional catalysts. They are chiral and have a powerful potential for combinatorial catalyst screening.[16,17] However, only a few examples of suitable ligands have been described in the literature. Those include bifunctional chelating reagents[18−20] developed for pharmaceutical applications, conjugates of lysine with EDTA or EDTA-related ligands,[21−23] as well as a bipyridine-modified alanine.[24] The only example of an acyclic tridentate amine ligand connected to an amino acid is a terpyridine derivative of cysteine, which has not been isolated as a monomer.[25,26]

Work in our laboratories has focused on the development and investigation of Werner-type coordination compounds with synthetic amino acids carrying well-defined metal binding sites.[27−29] In this report we present ligands derived from glycine, L-phenylalanine, and L-lysine. Zinc complexes have been prepared and investigated by X-ray crystallography, NMR, and circular dichroism spectroscopy. Characteristics of the compounds are the availability of suitable coupling positions for further derivatization, the interplay between the metal center and its chiral environment, as well as the availability of open coordination sites for metal-centered reactions.

Results

Ligand Synthesis

Our initial approach involved applying carboxylate-substituted tridentate amines in standard amide coupling reac-

[a] Institute for Inorganic Chemistry,
University of Erlangen-Nürnberg,
Egerlandstraße 1, 91058 Erlangen, Germany
Fax: (internat.) + 49-(0)9131/852-7387
E-mail: alsfassr@anorganik.chemie.uni-erlangen.de
[b] ITC-CPV, Forschungszentrum Karlsruhe,
Postfach 3640, 76021 Karlsruhe

  1434−1948/00/0808−1723 $ 17.50+.50/0

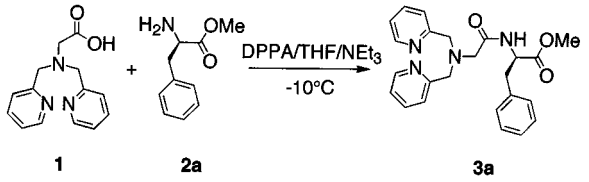

Scheme 1. Azide coupling strategy for the synthesis of the ligand **3a**

tions with the N-termini of amino acids (Scheme 1). The triamine used was the bis(picolyl)glycine **1**, which was prepared according to a procedure described by Que et al.[30] for the synthesis of iron complexes. Different methods were examined for coupling **1** to the amino group of L-phenylalanine methyl ester. Attempts to prepare the acid chloride by reaction of bis(picolyl)glycine with thionyl chloride failed. Formation of an amide bond by the intermediate formation of a mixed anhydride with isobutyl chlorofomate[31] also proved unsuccessful. The desired ligand L-bpaAc−Phe−OMe (**3a**) was finally obtained from **1** and phenylalanine methyl ester (**2a**) by the application of diphenylphosphoryl azide at low temperature in THF (Scheme 1).[31] However, purification of the product was difficult and the method afforded only poor yields (below 10%).

Since the coupling strategies described above were not satisfactory we changed our approach. The method employed involves bromoacetylation of an appropriate amino acid ester followed by nucleophilic substitution (Scheme 2). This coupling method has been shown to be very useful for the synthesis of polyfunctional chelating ligands. Typical examples include polyazamacrocycle−protein conjugates[32] for pharmaceutical applications and a phenylalanine−triazacyclononanetriamide derivative that served as a model for peptide organization at transition-metal templates.[33] Applications are not limited to metal-peptide derivatives, as exemplified by the synthesis of a hexadentate open-chain ligand by Sargeson et al.[34]

Scheme 2 illustrates our synthesis of L-bpaAc−Phe−OMe (**3a**) and the analogous ligand L-bpaAc−Lys(Z)−OMe (Z = benzyloxycarbonyl) (**3b**). L-Phe−OMe (**2a**) and L-Lys(Z)−OMe (**2b**) were treated with bromoacetyl bromide to yield the respective products L-BrAc−Phe−OMe (**4a**) and L-BrAc−Lys(Z)−OMe (**4b**). The synthesis of **4a** has been reported earlier in a communication by Fairlie et al.[33] but no experimental details were

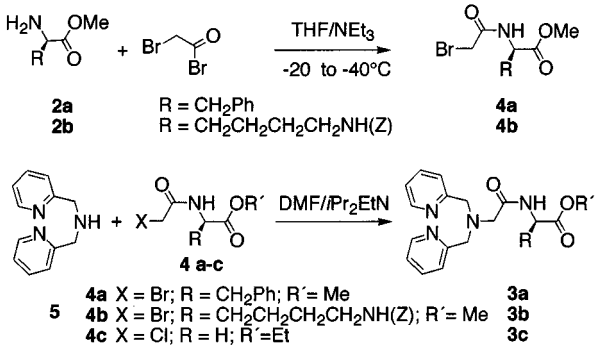

Scheme 2. Haloacetyl strategy for the synthesis of the ligands **3a**−**c**

given. Subsequent reaction of **4a** and **4b** with bis(picolyl)-amine (bpa, **5**) resulted in the formation of the desired chiral ligands **3a** and **3b**.

We have also prepared the nonchiral glycine derivative **3c** (Scheme 2) for comparative studies concerning the role of the chiral ligand environments provided by **3a** and **3b**. The starting material for this synthesis was commercially available (chloroacetyl)glycine. It turned out that the yields of its reaction with **5** (ca. 50%) are significantly lower than those obtained after bromide substitution even if both steps of the bromoacetyl bromide route are considered (overall yield ca. 80%). All three ligands were conveniently purified by flash column chromatography and obtained as spectroscopically pure (^{1}H NMR) yellow oils, which were further characterized by FD-MS.

Complexes

The amino acid ligands **3a**−**c** readily react with nonaqueous zinc triflate [Zn(OTf)$_2$] in dry acetonitrile (Scheme 3). Single crystals suitable for X-ray crystallographic characterization were obtained for [(bpaAc−Gly−OEt)ZnOTf]OTf (**6c**) (Figure 1). The initially formed triflate complexes **6a**−**c** are extremely moisture-sensitive and hygroscopic. Their hydrolysis products **7a**−**c** are readily obtained in the presence of moisture from solvents or air. Single crystals of the aquo complex [(L-bpaAc−Phe−OMe)(H$_2$O)Zn](OTf)$_2$ (**7a**, Figure 2) were obtained from dichloromethane/ethyl ether solutions of **6a**, which were exposed to air. Accordingly, it is difficult to obtain samples that do not show at least trace amounts of water in their NMR spectra. C,H,N elemental analysis data are also consistent with the presence of various amounts of water. However, the monocations [LZnOTf]$^+$ are the dominant species observed by FAB mass spectrometry for all complexes.

It is interesting to note that the glycine derivative **6c** was found to be the least moisture-sensitive whereas we were not able to obtain a dry sample of the L-bpaAc−Lys(Z)−OMe complex **6b**. Purification of the latter was further complicated because the compound always separates as an oil regardless of the solvent applied, thereby

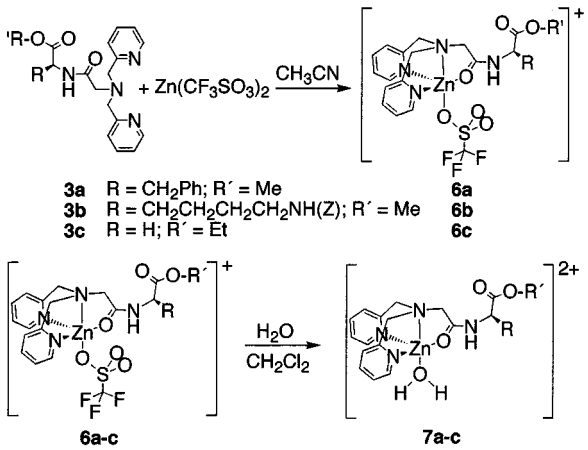

Scheme 3. Synthesis and structures of the zinc complexes **6a**−**c** and **7a**−**c**

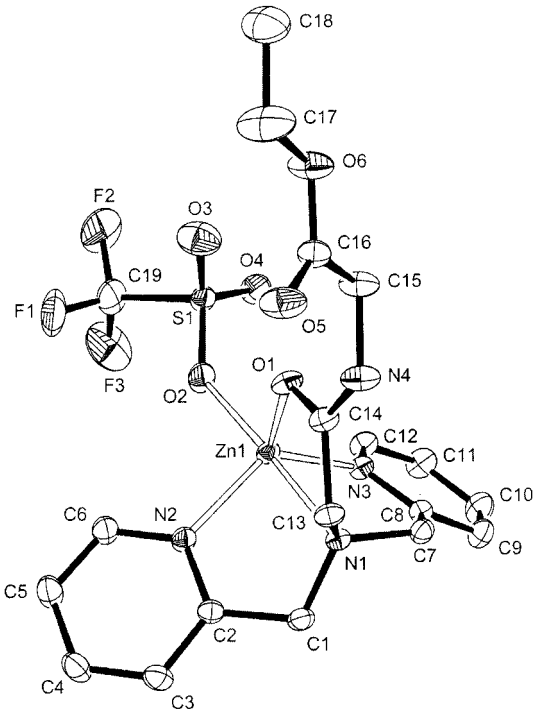

Figure 1. X-ray structure of the cation [(bpaAc−Gly−OEt)(OTf)Zn]$^+$ (**6c**, H atoms omitted for clarity)

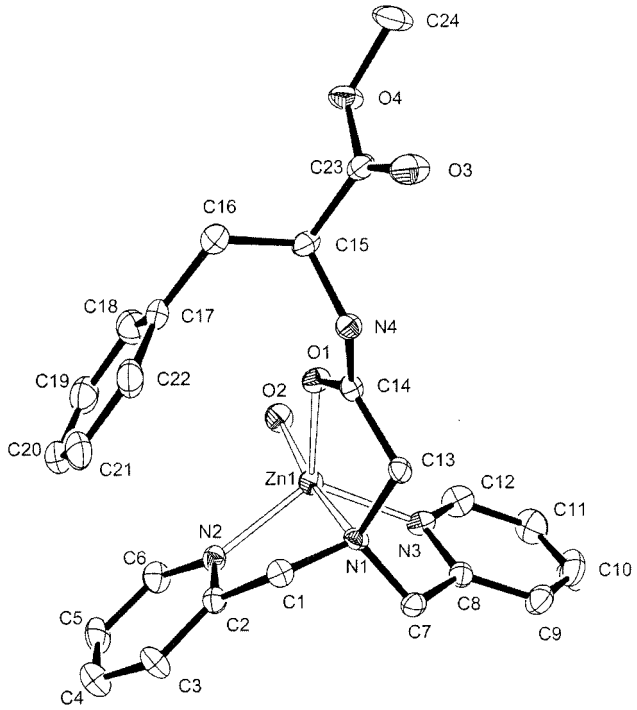

Figure 2. X-ray structure of the cation [(bpaAc−Phe−OMe)(H_2O)Zn]$^{2+}$ (**7a**, H atoms omitted for clarity)

preventing recrystallization. The oil solidified as a white foam upon drying under vacuum and this was characterized by NMR, IR, and circular dichroism spectroscopy, as well as by FAB-MS. The spectroscopic properties of this compound compare well with those of complexes **7a** and **7c** thus ensuring a correct interpretation of the data, which are consistent with the formulation **7b** given in Scheme 3.

Table 1. Selected bond lengths [Å] and angles [°] for the complexes **6c** and **7a**

	6c	**7a**
Zn(1)−O(2)	2.0145(18)	1.990(3)
Zn(1)−O(1)	2.0197(I8)	2.054(2)
Zn(1)−N(2)	2.039(2)	2.046(3)
Zn(1)−N(3)	2.060(2)	2.057(3)
Zn(1)−N(1)	2.1883(19)	2.189(3)
O(2)−Zn(1)−O(1)	99.29(9)	92.52(12)
O(2)−Zn(1)−N(2)	97.06(8)	105.96(15)
O(1)−Zn(1)−N(2)	113.13(8)	113.12(11)
O(2)−Zn(1)−N(3)	102.36(8)	101.59(15)
O(1)−Zn(1)−N(3)	116.84(8)	113.91(11)
N(2)−Zn(1)−N(3)	121.80(8)	123.42(13)
O(2)−Zn(1)−N(1)	176.93(8)	170.40(13)
O(1)−Zn(1)−N(1)	80.68(7)	78.45(10)
N(2)−Zn(1)−N(1)	80.18(8)	80.87(11)
N(3)−Zn(1)−N(1)	80.32(8)	79.48(12)

Solid-State Structures

The mononuclear cation of [L-bpaAc−Gly−OEt)Zn(OTf)](OTf) (**6c**) is shown in Figure 1. Selected bond lengths and angles are summarized in Table 1. A slightly distorted trigonal bipyramidal coordination environment at Zn^{2+} is observed with one triflate anion and the bridging tertiary amine nitrogen atom occupying the axial positions (N−Zn−O = 177°). The two pyridine N atoms and the amide oxygen atom of the amino acid ligands are bound in the trigonal plane. A comparison with zinc complexes of tris(picolyl)amine[35] and bis(picolyl)glycine,[36] respectively, confirms that the equatorial pyridine N−Zn bonds (204−206 pm), as well as the longer axial N−Zn bond (219 pm) are typical for tripodal quadridentate ligands derived from bis(picolyl)amine. In contrast, all Zn−N bonds are equal in trigonal-bipyramidal[37] and octahedral[38] zinc complexes of the tridentate bis(picolyl)amine ligand itself. The amide and triflate O−Zn distances in **6** (CO: 202 pm; OTf: 201 pm) are in excellent agreement with those found for carboxylate O−Zn bonds in bis(picolyl)glycine complexes.[36]

Facile exchange of a triflate ligand is an expected property of the complexes **6a**−**c**. When a sample of [(L-bpaAc−Phe−OMe)Zn(OTf)](OTf) (**6a**) in CH_2Cl_2/Et_2O was exposed to moist air overnight, crystals of the dicationic aquo complex [(L-bpaAc−Phe−OMe)(H_2O)Zn](OTf)$_2$ (**7a**, Figure 2 and Table 1) were obtained. A slight tetragonal distortion of its trigonal bipyramidal geometry is evident from the 170° angle between the coordinated water molecule, Zn^{2+}, and the tertiary amine nitrogen atom. The axial oxygen ligand is tilted towards the amide oxygen atom [**7a**: H_2O−Zn−O = 92°/H_2O−Zn−N(equatorial) = 102−106° compared with **6**: OTf−Zn−O = 99° OTf−Zn−N(equatorial) = 97−102°].

As can be seen from Figure 1 and 2 the ester functions of the ligands are noncoordinating and available for further derivatization. An interesting feature of the chiral phenyl-

alanine ligand in **7a** is the orientation of its phenyl ring. The ring covers one side of the open coordination site between the amide oxygen atom and one of the pyridine rings with its center located 4.5 Å away from the metal center. The possible formation of a chiral pocket is an important difference between **3a**/**3b** and comparable ligands developed by Canary et al.[39,40] These authors have synthesized chiral derivatives of tris(picolyl)amine by derivatization of the bridging methylene groups of the ligands leading to complexes in which the bulky substituents are always pointing away from the metal center.

The solid-state IR spectra (KBr pellets) of our compounds are consistent with the X-ray crystallographic results. Binding of the amide oxygen atom is evident from a red shift of the amide IR vibrations in the complexes compared with the free ligands [1672 (**3a**) → 1641 (**7a**); 1668 (**3b**) → 1637 (**7b**); 1674 (**3c**) → 1641 (**7c**)]. The spectra of all complexes exhibit signals for the triflate anions between 1200 and 1300 cm^{-1}. These values are typical for noncoordinating $CF_3SO_3^-$ and are consistent with the formulations **7a**−**7c**. A broad OH band at 3000 cm^{-1} was always observed.

NMR Spectra

The solid-state structure of **7a** suggests that the chiral environment provided by the phenylalanine moiety may influence the accessibility of the open coordination site of the metal centers. It is important for reactivity studies to probe this structural feature in solution. We selected diamagnetic Zn^{2+} complexes as a starting point for our investigations since they allow the application of NMR spectroscopy to compare solution and solid-state structures. The assignment of the ^{1}H-NMR signals of **7a**−**c** ($CDCl_3$ solutions) is based on comparison with the free ligands, the bromoacetylated compounds, and the starting materials, as well as ^{1}H-^{1}H and ^{1}H-^{13}C COSY spectra.

As may be expected the pyridine proton resonances are shifted to lower frequencies upon coordination of the metal ion. The two rings are equivalent in the free ligands **3a**−**c**, as well as in [(bpa-Gly−OEt)(H_2O)Zn]($OTf)_2$ (**7c**). A different pattern is observed in the spectra of the chiral complexes **7a** and **7b**. These compounds show two inequivalent pyridine rings with partially overlapping signals as a consequence of the chiral carbon center. The observed splitting is a clear indication of the structural rigidity induced by metal coordination.

A very sensitive probe for changes in the environment are the methylene proton resonances, which are shown in Figure 3. Unfortunately, some of the signals overlap with those of the methyl esters and α-CH groups but they are unambiguously assignable based on ^{1}H-^{1}H and ^{1}H-^{13}C COSY experiments as well as integration. The C(O)−CH_2 groups are observed as singlets in the ligands **3a**−**3c**. Their corresponding signals of the chiral complexes **7a** and **7b** are split into two doublets. The pyridine-CH_2 protons are diastereotopic in the chiral ligands **3a** and **3b** and their signals appear as AB systems with geminal coupling constants of ca. 14 Hz. These signals are further split in the

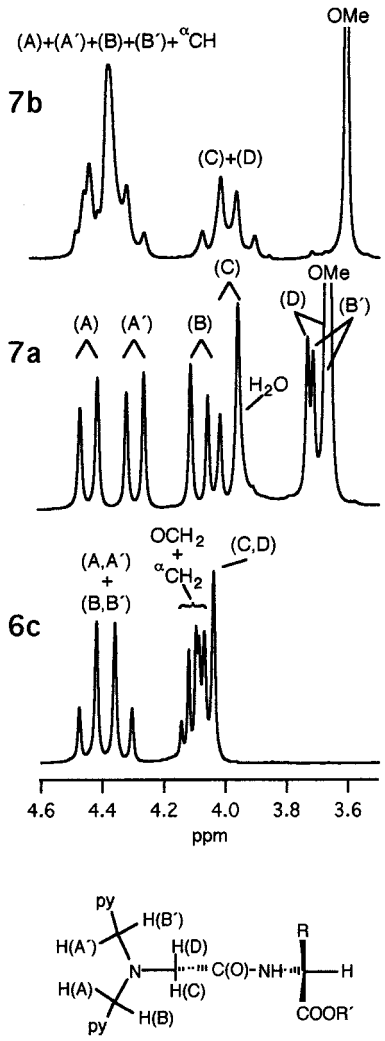

Figure 3. ^{1}H-NMR spectra of the zinc complexes **6c**, **7a**, and **7b** in $CDCl_3$

spectra of the complexes **7a** and **7b** since the two pyridine rings become inequivalent.

Most interesting is the ^{1}H-NMR spectrum of the phenylalanine derivative **7a**. Six doublets are observed for the six methylene protons. Two of them are observed at a significantly higher field (δ = 3.7) than expected if the other two complexes **7b** and **7c** are considered as a reference. The ^{1}H-^{1}H COSY spectrum confirms that one of these signals can be assigned to the C(O)−CH_2 group, whereas the other corresponds to a pyridine−methylene bridge. We interpret the observed high-field shift as an effect of the aromatic ring current of the phenyl ring, which is situated between one pyridine ring and the amide function (Figure 2). A corresponding high-field shift is also observed for the phenyl protons in **7a**, which are observed at rather unusual values of δ = 6.62 (H4) and δ = 6.92 (H3,5). The NMR spectra thus confirm the importance of specific interactions between the benzyl group of phenylalanine and the metal coordination sphere in **7a**.

Exchange of the coordinated triflate by water from air is also evident from NMR spectroscopy. For the extremely hygroscopic free ligands in $CDCl_3$ we occasionally observe

a signal at $\delta = 2$, which is assignable to H_2O. This signal is shifted to significantly lower fields in the complexes with values ranging up to $\delta = 5.6$ in the spectrum of [(L-bpa-Lys−OMe)(H_2O)Zn](OTf)$_2$ (**7b**). The position depends on the water content and moves towards $\delta = 2$ for higher H_2O concentrations. This is consistent with a fast equilibrium between coordinated and noncoordinated water molecules. It is interesting to note that the urethane H signals of the benzyloxycarbonyl protecting groups in **3b** and **7b** are sensitive to the presence of water and shift to slightly higher fields if the compounds are not rigorously dry. All other signals, including the amide H resonance, are invariant in $CDCl_3$ under all experimental conditions relevant for this work.

Circular Dichroism

Ordering phenomena of chiral molecules and supramolecules in solution are conveniently probed by circular dichroism spectroscopy.[41]–[49] A particular advantage of the method is its applicability where UV/Vis spectra are not very informative. The electronic absorption spectra of the bromoacetylated amino acids **4a** and **4b**, (chloroacetyl)glycine, the ligands **3a**−**3c**, as well as the zinc complexes **7a**−**7c** in methanol, show only a broad band at 260 nm, which is largely obscured by the slope of a strong absorption below 200 nm. In contrast, the CD spectra of [(L-bpaAc−Phe−OMe)(H_2O)Zn](OTf)$_2$ (**7a**, Figure 4a) and [(L-bpaAc−Lys−OMe)(H_2O)Zn](OTf)$_2$ (**7b**, Figure 4b) measured in methanol (10^{-3} M) have very distinct features that further support the data obtained from NMR and X-ray crystallographic studies.

The parent amino acids L-Lys−OMe and L-Phe−OMe display only one band at 210 nm (Lys) and 220 nm (Phe), respectively. The signal observed for phenylalanine is stronger and may be assigned to the π-π* transition of the phenyl ring. Bromoacetylation of ε-(benzyloxycarbonyl)lysine methyl ester results in a new signal with a negative Cotton effect at 225 nm and a positive Cotton effect at 245 nm. A shoulder at 245 nm is also well-resolved in the corresponding phenylalanine derivative. This feature disappears in the spectra of the two ligands **3a** and **3b** and a new band with a positive Cotton effect is observed at 260 nm. We assign this band to π-π* transitions of the pyridine rings in agreement with interpretations given by Canary et al.[40] Upon complexation with Zn^{2+} the sign of the pyridine signal changes and the band is shifted to slightly longer wavelengths. It is evident from Figure 4b that the intensity of the 220-nm band is significantly smaller for the ligand **3a** than for the other phenylalanine derivatives discussed in our study. This may be a consequence of the higher flexibility of L-bpaAc−Phe−OMe compared with either **2a**, **4a**, or **7a**. However, we do not have an obvious explanation for this behavior at the present stage of our investigations.

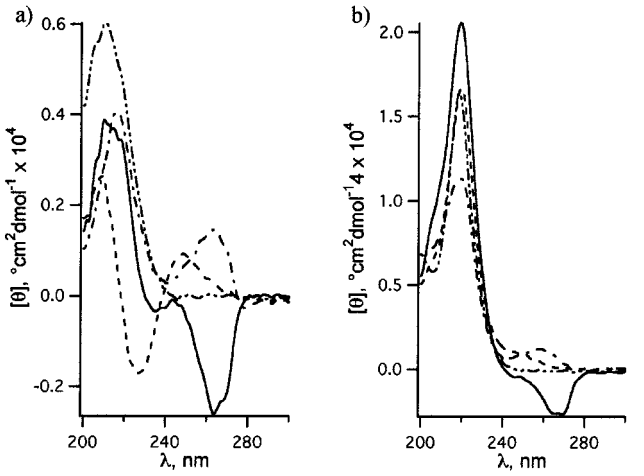

Figure 4. Circular dichroism spectra (10^{-3} M in methanol) of: (a) the L-lysine derivatives Lys(Z)−OMe (**2b**; − · · −), BrAc−Lys(Z)−OMe (**4b**; − −), bpaAc−Lys(Z)−OMe (**3b**; − · −), and [(bpaAc−Lys(Z)−OMe)(H_2O)Zn](OTf)$_2$ (**7b**, —); (b) the L-phenylalanine derivatives Phe−OMe (**2a**; − · · −), BrAc−Phe−OMe (**4a**; − −), bpaAc−Phe−OMe (**3a**; − · −), and [(bpaAc−Phe−OMe)(H_2O)Zn](OTf)$_2$ (**7a**; —)

The observed spectral changes associated with the pyridine ligands indicate that the interaction of the chromophore with its chiral environment is effected by complexation. This observation may be compared with the organization of peptides by metal ions[50] and the phenomenon of metal-induced circular dichroism.[48] It is interesting to note that the differential extinction coefficients observed in this work are comparable with values obtained for biomolecules such as proteins or DNA.[51]

Discussion

The ligands **3a**−**c** are quadridentate and readily bind zinc(II) to yield stable compounds that are soluble in a variety of solvents ranging from methanol to chloroform. A labile coordination site is available in the trigonal-bipyramidal triflate complexes **6a**−**c**. This is illustrated by the facile ligand exchange observed in the presence of moisture (air), which results in the formation of **7a**−**c**. We have designed our ligands with two features in mind. One is the availability of a functional group for further derivatization. This requirement is met by the presence of a noncoordinating ester function in the complexes **6a**−**c** and **7a**−**c**. No indication was found in the solid state or in solution for an interaction between this group and the metal center. Furthermore, the protected ε-amino group of lysine in bpa-Lys(Z)−OMe (**3b**) may be useful as an additional site for modifications.

Our second objective was to find a chiral noncoordinating environment provided by the ligands. The three amino acid derivatives used in the present study are well suited for comparative studies concerning interactions between the coordinated metal center and its noncoordinating environment since their side chains represent achiral and chiral, as well as aliphatic and aromatic substituents. In the solid-state structure of **7a** the phenyl ring of L-phenylalanine is oriented towards the open coordination site at Zn^{2+} (Figure 2) covering one side of the complex between a pyridine ring and the coordinated amide group. The NMR- and CD-spectroscopic studies presented in this report provide evi-

dence for a significant organization of the chiral environment upon metal complexation in **7a** and **7b** in solution. This is of particular interest for applications of the ligands and complexes in molecular recognition and reactivity studies.

Conclusions

The ligands **3a−c** are useful new building blocks for the synthesis of polyfunctional transition-metal complexes based on the chiral pool provided by natural amino acids. They bind tightly and in a well-defined manner to metal ions but offer sufficient flexibility and accessible open coordination sites for metal-ion reactivity. The amino acid side chains cover one side of the complexes such that the complexes **7a** and **7b** are promising candidates for enantioselective molecular recognition and hydrolysis studies. Our concept allows a facile and systematic modification of the properties of metal complexes by variation of the amino acid. The lysine derivative **7b** is particularly interesting for further modifications at the ε-amino group of the ligand. We are currently investigating this possibility in order to extend our building-block approach.

Experimental Section

General Methods: Spectra were recorded with the following instruments: UV/Vis: Cary 1G Spectrophotometer. − Circular Dichroism: Jasco J710 Spectropolarimeter. − IR: Mattson Polaris FT IR. − ^{1}H and ^{13}C NMR: Bruker Avance DPX 300. All chemical shifts are referenced to TMS as internal standard, with high-frequency shifts recorded as positive. − All reactions were carried out under dry nitrogen. The following workup was performed under ambient laboratory conditions unless stated otherwise. The bis(picolyl)glycine **1**[30] and bis(picolyl)amine **5**[52,53] were synthesized according to published procedures. L-Lys(Z)−OMe·HCl (**2b**) was purchased from Nova Biochem, L-Phe−OMe·HCl (**2a**) from Bachem. Absolute solvents (THF, CH_2Cl_2, Et_2O, DMF, CH_3CN) were purchased from Fluka and stored under nitrogen. Ethyl acetate and hexane were reagent grade (Roth). All solvents were used without further purification. Silca gel Merck type 9385 (230−400 mesh, 60 Å) from Aldrich was used for flash column chromatography. Eluents were optimized by TLC on silica gel 60 F254 sheets (0.2 mm layer) from Riedel-de Haën. All other chemicals including ClAc−Gly−OEt and deuterated solvents were obtained from Aldrich. Triethylamine was distilled under N_2 prior to use.

Diphenylphosphoryl Azide (DPPA) Coupling

bpaAc−Phe−OMe (3a): Freshly distilled NEt_3 (1.00 mL, 7.00 mmol) was added in one portion to a stirred suspension of **2a** × HCl (166 mg, 0.77 mmol) under N_2 in 10 mL of absolute THF. Stirring was continued for 30 min, the mixture filtered to remove NEt_3 × HCl and the resulting clear solution cooled to −10 °C using an ice/salt bath. This solution was added in one portion with stirring to another THF (10 mL) solution containing **1** (150 mg, 0.70 mmol) at −10 °C. DPPA (0.17 mL, 0.77 mmol) was added slowly followed by dropwise addition of NEt_3 (0.11 mL, 0.77 mmol). Care was taken to keep the temperature at or below −10 °C. The stirred reaction mixture was kept at −10 °C for another 30 min and the resulting solution was then allowed to warm up to room temperature. Stirring was continued overnight, all the solvent was removed under vacuum and the residue was treated with 10 mL of $CHCl_3$. Cooling to −20 °C afforded a solid, which was filtered off and discarded. The filtrate was concentrated to dryness and the solid obtained was redissolved in a minimum amount of AcOEt. This solution was purified by flash column chromatography on silica gel. Impurities eluted with AcOEt and the product was obtained with yields below 10% by subsequent elution with pure methanol.

Bromoacetylated Amino Acid Esters

BrAc−Phe−OMe (4a): L-Phe−OMe·HCl (10.00 g, 46.40 mmol) was suspended in 200 mL of THF. Triethylamine (12.93 mL, 92.80 mmol) was added with stirring and the mixture was cooled to −10 °C in an ice/salt bath. Bromoacetyl bromide (4.04 mL, 46.40 mmol) was dissolved in 50 mL of THF and the solution was added dropwise to the cold suspension over a period of 2 h. The mixture was stirred for another 2 h without further cooling. Insoluble $HNEt_3Br$ was filtered off and the solvent removed in a vacuum. The crude yellow solid obtained after removal of all THF was redissolved in the minimum amount of ethyl acetate. Colorless needles of the product **4a** (13.46 g, 44.86 mmol, 96.7%) were obtained after addition of hexane and storage in a refrigerator (−20 °C) overnight. The compound was collected on a sintered-glass filter, dried under vacuum, and characterized by FAB-MS, ^{1}H-NMR and ^{13}C-NMR spectroscopy. − FAB-MS (nitrobenzyl alcohol); *m/z*: 300 [M^+], 240 [M^+ − COOMe]. − ^{1}H NMR (300 MHz, $CDCl_3$): δ = 3.15 (m, 2 H, $^{\beta}CH_2$), 3.74 (s, 3 H, OCH_3), 3.84 (s, 2 H, Br−CH_2), 4.85 (m, 1 H, $^{\alpha}CH$), 6.83 (s, br, 1 H, NH), 7.12 (m, 2 H, H2-Ph + H6-Ph), 7.28 (m, 3 H, H3-Ph + H4-Ph + H5-Ph). − ^{13}C NMR (75 MHz, $CDCl_3$): δ = 28.6 (Br−C), 37.7 ($^{\beta}C$), 52.5 (OCH_3), 53.7 ($^{\alpha}C$), 127.3, 128.7, 129.3 (C2-Ph + C3-Ph + C4-Ph + C5-Ph + C6-Ph), 135.9 (C1-Ph), 165.2, 171.3 [C(O)-ester + C(O)-amide]. − IR (KBr): $\tilde{\nu}$ = 1734 cm^{-1} (COOMe), 1645 (amide I), 1537 (amide II). − Circular Dichroism (10^{-3} M in methanol): λ, nm ([θ] × 10^4 °cm^2dmol^{-1}) = 219 (+1.67), 244 (shoulder, +0.11).

BrAc−Lys(Z)−OMe (4b): L-Lys(Z)−OMe·HCl (5.02 g, 15.20 mmol) was suspended in 150 mL of THF and cooled to −30 °C in a methanol/dry ice bath. Triethylamine (4.22 mL, 30.40 mmol) was added and the mixture stirred for 30 min. Bromoacetyl bromide (1.32 mL, 15.20 mmol) was dissolved in 50 mL of THF and the solution added dropwise to the cold suspension over a period of 2.5 h. The mixture was stirred for another 1.5 h at −30 °C. Insoluble $HNEt_3Br$ was filtered off and the solvent removed by rotary evaporation. The crude brown solid obtained after removal of all THF was redissolved in 50 mL of hot ethyl acetate and the solution left at −20 °C overnight. The product precipitated as a colorless solid, which was filtered off and dried under vacuum. A second crop was obtained after addition of hexane and subsequent cooling. The fractions were combined (5.51 g, 13.27 mmol, 87.3%) and characterized by FAB-MS, ^{1}H-NMR and ^{13}C-NMR spectroscopy. − FD-MS ($CDCl_3$); *m/z*: 415 [M^+]. − ^{1}H NMR (300 MHz, $CDCl_3$): δ = 1.38 (m, 2 H, $^{\gamma}CH_2$), 1.52 (m, 2 H, $^{\delta}CH_2$), 1.81 (m, 2 H, $^{\beta}CH_2$), 3.18 (m, 2 H, $^{\varepsilon}CH_2$), 3.75 (s, 3 H, OCH_3), 3.87 (s, 2 H, Br−CH_2), 4.57 (m, 1 H, $^{\alpha}CH$), 4.89 (m, 1 H, NH-Z), 5.09 (s, 2 H, CH_2-Z), 7.35 (m, 5 H, Ph-Z), 7.02 (d, 1 H, $^3J_{HH}$ = 7.3 Hz, NH). − ^{13}C NMR (75 MHz, $CDCl_3$): δ = 22.2 ($^{\gamma}C$), 28.7 (Br−C), 29.4 ($^{\delta}C$), 31.7 ($^{\beta}C$), 40.47 ($^{\varepsilon}C$), 52.6 (OCH_3 + $^{\alpha}C$), 66.7 (CH_2-Z), 128.1, 128.1, 128.4, 128.5 (Z-C2-Ph + Z-C3-Ph + Z-C4-Ph + Z-C5-Ph + Z-C6-Ph), 136.6 (Z-C1-Ph), 156.5 [Z-C(O)], 165.6, 172.2 [C(O)-ester + amide]. − IR (KBr): $\tilde{\nu}$ = 1740 cm^{-1} (COOMe), 1698 (Z-urethane), 1646 (amide I), 1540 (amide II). − Circular Dichroism

(10^{-3} M in methanol): λ, nm ([θ] × 10^4 °cm^{2}dmol^{-1}) = 209 (+0.26), 227 (−0.17), 248 (+0.09).

Ligands

General Procedure: Equimolar amounts of bis(picolyl)amine (**5**), the respective haloacetylated amino acid ester, and ethyldiisopropylamine (DIPEA) were dissolved in DMF. The solution was stirred for 20 h at room temperature. All solvents were removed by rotary evaporation. Ethyl acetate was added, resulting in the precipitation of the ammonium halide salt, which was filtered off and discarded. The filtrate was concentrated to dryness yielding a brown oil, which was purified by silica gel column chromatography using CH_2Cl_2/MeOH (11:1) as eluent. A small yellow fraction containing some of the haloacetylated amino acid ester starting material eluted first. The product was eluted next as a broad light yellow (yellow in the case of **3a**) fraction. A third yellow fraction, which was well separated from the product, was usually not collected. The solution containing the desired product was concentrated to dryness by rotary evaporation and the resulting light yellow oil dried under vacuum.

bpaAc−Phe−OMe (3a): 9.00 g (29.98 mmol) of **4a**, 5.91 g (29.98 mmol) of bpa, 5.20 mL (29.98 mmol) of DIPEA, 100 mL of DMF, 100 mL of AcOEt. Yield: 10.17 g (24.31 mmol, 81%). − $C_{24}H_{26}N_4O_3$ (418.5 g/mol): FD-MS ($CDCl_3$); *m/z*: 418 [M^+]. − ^{1}H NMR (300 MHz, $CDCl_3$): δ = 2.00 (H_2O), 3.12−3.29 (ABX, 2 H, $^{\beta}CH_2$), 3.26 [s, 2 H, C(O)−CH_2], 3.69 (s, 3 H, OCH_3), 3.73, 3.85 (2 × d, 4 H, $^2J_{HH}$ = 14.2 Hz, 2 × py-CH_2), 4.90 (m, 1 H, $^{\alpha}CH$), 7.18 (m, 9 H, 5 × H-Ph + H3-py + H5-py), 7.56 (m, 2 H, H4-py), 8.52 (d, 2 H, $^3J_{HH}$ = 4.9 Hz, H6-py), 9.05 (d, 1 H, $^3J_{HH}$ = 8.0 Hz, NH). − ^{13}C NMR (75 MHz, $CDCl_3$): δ = 37.5 ($^{\beta}C$), 52.1 (OCH_3), 53.1 ($^{\alpha}C$), 57.6 [C(O)−CH_2], 60.1 (py-CH_2), 122.3, 122.9 (C3-py + C5-py), 126.80, 128.4, 129.2 (C2-Ph + C3-Ph + C4-Ph + C5-Ph + C6-Ph), 136.5 (3 C, 2 × C4-py + C1-Ph), 149.1 (C6-py), 158.2 (C2-py), 171.2, 172.1 [C(O)-ester + C(O)-amide]. − IR (film on NaCl): $\tilde{\nu}$ = 1745 cm^{-1} (COOMe), 1672 (amide I), 1513 (amide II). − Circular Dichroism (10^{-3} M in methanol): λ, nm ([θ] × 10^4 °cm^{2}dmol^{-1}) = 221 (+1.13), 257 (+0.05), 265 (+0.13).

bpaAc−Lys(Z)−OMe (3b): 1.83 g (4.41 mmol) of **4b**, 877 mg (4.41 mmol) of bpa, 0.77 mL (4.41 mmol) of DIPEA, 50 mL of DMF, 30 mL of AcOEt. Yield: 1.67 g (3.13 mmol, 71%). − $C_{29}H_{35}N_5O_5$ (533.6 g/mol): FD-MS ($CDCl_3$); *m/z*: 534 (M^+). − ^{1}H NMR (300 MHz, $CDCl_3$): δ = 1.39 (m, 2 H, $^{\gamma}CH_2$), 1.51 (m, 2 H, $^{\delta}CH_2$), 1.85 (m, 2 H, $^{\beta}CH_2$), 3.12 (m, 2 H, $^{\varepsilon}CH_2$), 3.35 [s, 2 H, C(O)−CH_2], 3.67 (s, 3 H, OCH_3), 3.78, 3.86 (2 × d, 4 H, $^2J_{HH}$ = 9.7 Hz, 2 × py-CH_2), 4.60 (m, 1 H, $^{\alpha}CH$), 5.06 (s, 2 H, Z-CH_2), 5.21 (m, 1 H, Z-NH), 7.14 (dd, 2 H, H5-py), 7.32 (m, 7 H, Z-Ph + H3-py), 7.60 (dd, 2 H, H4-py), 8.53 (d, 2 H, $^3J_{HH}$ = 4.56 Hz, H6-py), 9.22 (d, 1 H, $^3J_{HH}$ = 7.3 Hz, NH). − ^{13}C NMR (75 MHz, $CDCl_3$): δ = 22.7 ($^{\gamma}C$), 29.3 ($^{\delta}C$), 31.7 ($^{\beta}C$), 40.7 ($^{\varepsilon}C$), 51.7, 52.0 (OCH_3 + $^{\alpha}C$), 57.8 [C(O)−CH_2], 60.5 (py-CH_2), 66.4 (Z-CH_2), 122.4, 123.1 (C3-py + C5-py), 128.0, 128.1, 128.3, 128.4 (Z-C2-Ph + Z-C3-Ph + Z-C4-Ph + Z-C5-Ph + Z-C6-Ph), 136.6 (2 C, Z-C1-Ph + C4-py), 149.2 (C6-py), 156.4, 158.3 [C(O)-Z + C2-py], 171.5, 172.8 [C(O)-ester + C(O)-amide]. − IR (film on NaCl): $\tilde{\nu}$ = 1741 cm^{-1} (COOMe), 1718 (Z-urethane), 1668 (amide I), 1529 (amide II). − Circular Dichroism (10^{-3} M in methanol): λ, nm ([θ] × 10^4 °cm^{2}dmol^{-1}) = 216 (+0.40), 263 (+0.15).

bpaAc−Gly−OEt (3c): 7.87 g (43.81 mmol) of ClAc−Gly−OEt; 8.72 g (43.81 mmol) of dpa, 7.65 mL (43.81 mmol) of DIPEA, 100 mL of DMF, 100 mL of AcOEt. Yield: 6.04 g (17.60 mmol, 40%). − $C_{18}H_{22}N_4O_3$ (342.4 g/mol): FD-MS ($CDCl_3$); *m/z*: 342 [M^+]. − ^{1}H NMR (300 MHz, $CDCl_3$): δ = 1.24 (t, 3 H, $^3J_{HH}$ = 7.1 Hz, OCH_2CH_3), 2 (H_2O), 3.37 [s, 2 H, C(O)−CH_2], 3.90 (s, 4 H, py-CH_2), 4.08 (d, 2 H, $^3J_{HH}$ = 5.9 Hz, $^{\alpha}CH_2$), 4.18 (q, 2 H, $^3J_{HH}$ = 7.1 Hz, OCH_2CH_3), 7.16 (dd, 2 H, H5-py), 7.35 (d, 2 H, H3-py), 7.63 (m, 2 H, H4-py), 8.55 (d, 2 H, H6-py), 9.07 (m, 1 H, NH). − ^{13}C NMR (75 MHz, $CDCl_3$): δ = 14.1 (OCH_2CH_3), 41.0 ($^{\alpha}C$), 57.9 [C(O)−CH_2], 60.2 (py-CH_2), 61.1 (OCH_2CH_3), 122.4 (C3-py), 123.3 (C5-py), 136.6 (C4-py), 149.2 (C6-py), 158.3 (C2-py), 169.8, 171.8 [C(O)-ester + C(O)-amide]. − IR (film on NaCl): $\tilde{\nu}$ = 1747 cm^{-1} (COOEt), 1674 (amide I), 1525 (amide II).

Zn Complexes

General Procedure: Solid $Zn(OTf)_2$ was added in one portion to a stirred solution of 1 equiv. of the respective ligand in CH_3CN. Stirring was continued overnight at room temp. followed by removal of all solvent under vacuum. CH_2Cl_2 was added to the residue and the resulting suspension left in a refrigerator (−20 °C) overnight. Unchanged $Zn(OTf)_2$ precipitated and was filtered off. In the case of **7b** the solvent was removed by rotary evaporation and the residue dried under vacuum. Further purification was not possible since the compound did not precipitate but rather separated as an oil from common organic solvents. Accordingly, the reported yield refers to the crude product. The two other complexes (**6c** and **7a**) were purified by addition of Et_2O to the clear CH_2Cl_2 filtrate and recrystallization at −20 °C. These complexes precipitated overnight as colorless microcrystalline solids. Yields are reported for recrystallized samples. It is evident from C,H,N analysis and NMR data that the bpaAc−Gly−OEt complex **6c** was isolated without significant amounts of coordinated water whereas the same workup affords the corresponding aquo complex **7a** for bpaAc−Phe−OMe. Single crystals suitable for X-ray structure analysis of **6c** and **7a** were obtained by slow recrystallization of the pure complexes from CH_2Cl_2/Et_2O at −20 °C under dry nitrogen over a period of several weeks.

[(bpaAc−Gly−OEt)(OTf)Zn](OTf) (6c): 426 mg (1.24 mmol) of **5**, 416 mg (1.24 mmol) of $Zn(OTf)_2$, 10 mL of CH_3CN, 10 mL of CH_2Cl_2. Yield: 573 mg (0.81 mmol, 65%). − $C_{20}H_{22}F_6N_4O_9S_2Zn$ (705.9 g/mol): calcd. C 34.03, H 3.14, N 7.94; found C 33.85, H 3.25, N 7.74. − FAB-MS (nitrobenzyl alcohol); *m/z*: 555 (**3c**-ZnOTf$^+$), 407 (**3c**-Zn$^+$). − ^{1}H NMR (300 MHz, $CDCl_3$): δ = 1.21 (t, 3 H, $^3J_{HH}$ = 7.1 Hz, OCH_2CH_3), 4.04 [s, 2 H, C(O)−CH_2], 4.10 (m, 4 H, $^{\alpha}CH_2$, OCH_2CH_3), 4.34, 4.44 (2 × d, 4 H, $^2J_{HH}$ = 5.6 Hz, 2 × py-CH_2), 7.63 (m, 4 H, H5-py + H3-py), 8.05 (m, 2 H, H4-py), 8.92 (d, 2 H, H6-py), 9.03 (m, 1 H, NH). − ^{13}C NMR (75 MHz, $CDCl_3$): δ = 13.9 (OCH_2CH_3), 42.4 ($^{\alpha}C$), 56.2 [C(O)−CH_2], 57.8 (py-CH_2), 61.8 (OCH_2CH_3), 120.2 (q, $^1J_{CF}$ = 301.9 Hz, OTf^-), 125.3, 125.9 (C3-py, C5-py), 141.9 (C4-py), 149.2 (C6-py), 154.3 (C2-py), 167.5, 174.3 [C(O)-ester + C(O)-amide]. − IR (KBr): $\tilde{\nu}$ = 1747 cm^{-1} (COOEt), 1641 (amide I), 1245 (CF_3SO_3), 1218 (CF_3SO_3).

[(bpaAc−Phe−OMe)(H_2O)Zn](OTf)$_2$ (7a): 743 mg (1.77 mmol) of **3a**, 643 mg (1.77 mmol) of $Zn(OTf)_2$, 15 mL of CH_3CN, 15 mL of CH_2Cl_2. Yield: 964 mg (1.20 mmol, 68%). − $C_{26}H_{28}F_6N_4O_{10}S_2Zn$ (800.0 g/mol): calcd. C 39.03, H 3.53, N 7.00; found C 38.94, H 3.53, N 6.82. − FAB-MS (nitrobenzyl alcohol); *m/z*: 631 (**3a**-ZnOTf$^+$), 481 (**3a**-Zn$^+$). − ^{1}H NMR (300 MHz, $CDCl_3$): δ = 2.84, 3.23 (ABX, 2 H, $^{\beta}CH_2$), 3.66 (s, 3 H, OCH_3), 3.67 [d, 1 H, $^2J_{HH}$ = 16.8 Hz, py-CH(A′)*H*(B′)], 3.70 [d, 1 H, $^2J_{HH}$ = 16.8 Hz, C(O)−CH(C)*H*(D)], 3.98 [d, 3 H, $^2J_{HH}$ = 16.8 Hz, C(O)−C*H*(C)H(D) + H_2O], 4.08 [d, 1 H, $^2J_{HH}$ = 16.8 Hz, py-CH(A)*H*(B)], 4.29 [d, 1 H, $^2J_{HH}$ = 16.8 Hz, py-CH(*A′*)H(B′)], 4.44 [d, 1 H, $^2J_{HH}$ = 16.8 Hz, py-CH(*A*)H(B)], 4.99 (m, 1 H, $^{\alpha}CH$), 6.62 (dd, 1 H, H4-Ph), 6.98 (dd, 2 H, H3,5-Ph), 7.19 (d, 2 H, H2,6-Ph),

Table 2. Details of crystal structure analyses

Compound	**6c**	**7a**
Empirical formula	$C_{20}H_{21}F_6N_4O_9S_2Zn$	$C_{26}H_{26}F_6N_4O_{10}S_2Zn \cdot H_2O$
Molecular mass	704.90	816.01
Temperature	200(2) K	200(2) K
Wavelength [Å]	0.71073	0.71073
Crystal system	monoclinic	monoclinic
Space group	$P2_1/n$	$P2_1$
a [Å]	15.4015(8)	13.8284 (18)
b [Å]	9.2332(5)	9.4051(19)
c [Å]	21.0333(11)	14.290(3)
β [°]	108.1050(10)	106.426(18)
Volume [Å^3]	2843.0(3)	1782.7(6)
Z	4	2
Calculated density	1.647 Mg/m^3	1.520 Mg/m^3
Absorption coefficient	1.104 mm^{-1}	0.896 mm^{-1}
F(000)	1428	832
Crystal size [mm]	0.4 × 0.2 × 0.2	0.25 × 0.15 × 0.15
θ range [°]	1.96−28.36	1.54−28.30
Index ranges	$-20 \le h \le 20$ $-12 \le k \le 11$ $-28 \le l \le 27$	$-18 \le h \le 18$ $-12 \le k \le 12$ $-18 \le l \le 18$
Reflections collected/unique	28766/6920	19429/8552
Refinement method	based on F^2	based on F^2
Data/restr./parameters	6920/0/388	8552/1/473
Goodness-of-fit on F^2	1.087	0.886
Final R indices [$I > 2\sigma(I)$]	$R1$ = 0.0410 $wR2$ = 0.1135	$R1$ = 0.0423 $wR2$ = 0.0697
R indices (all data)	$R1$ = 0.0549 $wR2$ = 0.1203	$R1$ = 0.1026 $wR2$ = 0.0806
Largest diff. peak and hole	0.874 and −1.065 eÅ^{-3}	0.361 and −0.411 Å^{-3}

7.62 (m, 4 H, H3-py + H5-py), 8.01, 8.08 (2 × m, 2 H, H4-py), 8.83, 8.85 (2 × m, 2 H, H6-py), 9.02 (d, 1 H, $^3J_{HH}$ = 8.6 Hz, NH). − ^{13}C NMR (75 MHz, $CDCl_3$): δ = 37.87 ($^{\beta}$C), 52.74 (OCH_3), 55.28 ($^{\alpha}$C), 56.04 [C(O)−CH_2], 57.58, 57.68 (py−CH_2), 120.21 (q, $^1J_{CF}$ = 317 Hz, OTf$^-$), 125.12, 125.36, 125.73 (2 × C3-py + 2 × C5-py), 126.42, 128.01, 129.74 (C2-Ph + C3-Ph + C4-Ph + C5-Ph + C6-Ph), 135.76 (C1-Ph), 141.71, 141.79 (2 × C4-py) 148.97, 149.04 (2 × C6-py), 154.25, 154.30 (2 × C2-py), 169.78, 173.46 [C(O)-ester + amide]. − IR (KBr): $\tilde{\nu}$ = 1749 cm^{-1} (COOMe), 1633 (amide I), 1284 (CF_3SO_3), 1245 (CF_3SO_3). − Circular Dichroism (10^{-3} M in methanol): λ, nm ([θ] × 10^4 °cm^{2}dmol^{-1}) = 219 (+2.05), 246 (−0.05), 265 (−0.26), 270 (−0.26).

[(bpa-Lys(Z)−OMe)(H_2O)Zn]($OTf)_2$ (7b): 131 mg (0.25 mmol) of **3b**, 91 mg (0.25 mmol) of $Zn(OTf)_2$, 10 mL of CH_3CN, 5 mL of CH_2Cl_2. Yield: 161 mg (0.19 mmol, 76%). − FAB-MS (nitrobenzyl alcohol); *m/z*: 746 (**3b**-ZnOTf$^+$), 596 (**3b**-Zn$^+$). − ^{1}H NMR (300 MHz, $CDCl_3$): δ = 1.20 (m, 2 H, $^{\gamma}CH_2$), 1.46 (m, 2 H, $^{\delta}CH_2$), 1.73 (m, 2 H, $^{\beta}CH_2$), 3.07 (m, 2 H, $^{\varepsilon}CH_2$), 3.67 (s, 3 H, OCH_3), 3.93, 4.04 [2 × d, 2 H, $^2J_{HH}$ = 17.4 Hz, C(O)−CH_2], 4.38 (m, 5 H, 2 × py-CH_2 + $^{\alpha}$CH), 5.07 (s, 2 H, CH_2-Z), 5.21 (m, 1 H, NH-Z), 7.35 (m, 5 H, Ph-Z), 7.54 (m, 4 H, 2 × H3-py + 2 × H5-py), 8.00 (m, 2 H, 2 × H4-py), 8.80 (m, 3 H, 2 × H6-py + NH). − ^{13}C NMR (75 MHz, $CDCl_3$): δ = 22.4 ($^{\gamma}$C), 29.0 ($^{\delta}$C), 30.5 ($^{\beta}$C), 40.4 ($^{\varepsilon}$C), 52.6 (OCH_3), 53.9 ($^{\alpha}$C), 56.9 [C(O)−CH_2], 58.8 (py-CH_2), 67.9 (Z-CH_2), 120.1 (q, $^1J_{CF}$ = 323 Hz, OTf$^-$), 125.1, 125.6 (C3-py + C5-py), 127.8, 128.0, 128.5 (5 C, Z-C2-Ph + Z-C3-Ph + Z-C4-Ph + Z-C5-Ph + Z-C6-Ph), 136.8 (2 C, Z-C1-Ph), 141.4 (C4-py), 148.6 (C6-py), 154.0 (C2-py), 156.8 [C(O)-Z], 170.6, 173.3 [C(O)-ester + C(O)-amide]. − IR (KBr): $\tilde{\nu}$ = 1745 cm^{-1} (COOMe), 1708 (Z-urethane), 1637 (amide I), 1283 (CF_3SO_3), 1253 (CF_3SO_3). − Circular Dichroism (10^{-3} M in methanol): λ, nm ([θ] × 10^4 °cm^{2}dmol^{-1}) = 213 (+0.37), 235 (−0.03), 264 (−0.26), 269 (−0.26).

X-ray Data Collection and Structure Refinement Details: Crystal data and experimental conditions are listed in Table 2. The molecular structures are illustrated in Figures 1 and 2. Selected bond lengths and bond angles with standard deviations in parentheses are presented in Table 1. Intensity data were collected with a Siemens SMART 5000 CCD-Diffractometer with graphite-monochromated Mo-K_α radiation (λ = 0.71073 Å). The exposure time was 10 s per frame collected with the ω-scan technique (Δω = 0.3°). The collected reflections were corrected for Lorentz, polarization and absorption effects. The structures were solved by direct methods and refined by full-matrix least-squares methods on F^2.[54]−[56] Non-hydrogen atoms were refined with anisotropic thermal parameters in both structures. The hydrogen atoms of the coordinated water molecule and the amide hydrogen atom of **7a** were localized from the difference electron density map and refined with isotropic thermal parameters. All other hydrogen atoms were fixed in geometrically calculated positions and isotropically refined. Details of the crystal structure determinations have been deposited at the Cambridge Crystallographic Data Centre as supplementary publication nos. CCDC-140521 (**6c**) and -140522 (**7a**). Copies of the data can be obtained free of charge on application to CCDC, 12 Union Road, Cambridge CB2 1EZ, U.K. [Fax: (internat.) + 44-1223/336-033; E-mail: deposit@ccdc.cam.ac.uk].

Acknowledgments

The authors gratefully acknowledge financial support from the Deutsche Forschungsgemeinschaft. We thank Prof. Rudi van Eldik who generously let us share his equipment, laboratory space, and

funding. We also thank Dr. Reiner Waibel at the Institute for Pharmacy and Food Chemistry, University of Erlangen, for his help with the circular dichroism measurements.

[1] E. Uhlmann, A. Peyman, G. Breipohl, D. W. Will, *Angew. Chem.* **1998**, *110*, 2954−2983.
[2] D. K. Smith, F. Diederich, *Chem. Eur. J.* **1998**, *4*, 1353−1361.
[3] X. Cha, K. Ariga, T. Kunitake, *J. Am. Chem. Soc.* **1996**, *118*, 9545−9551.
[4] T. Lescrinier, C. Hendrix, L. Kerremans, J. Rozenski, A. Link, B. Samyn, A. van Aerschot, E. Lescrinier, R. Eritja, J. van Beeumen, P. Herdewijn, *Chem. Eur. J.* **1998**, *4*, 425−433.
[5] N. Voyer, J. Lamothe, *Tetrahedron* **1995**, *51*, 9241−9284.
[6] J. P. Schneider, J. W. Kelly, *Chem. Rev.* **1995**, *95*, 2169−2187.
[7] T. Hohsaka, D. Kajihara, Y. Ashizuka, H. Murakami, M. Sisido, *J. Am. Chem. Soc.* **1999**, *121*, 34−40.
[8] E. Graf von Roedern, E. Lohof, G. Hessler, M. Hoffmann, H. Kessler, *J. Am. Chem. Soc.* **1996**, *118*, 10156−10167.
[9] B. Imperiali, R. S. Roy, *J. Am. Chem. Soc.* **1994**, *116*, 12083−12084.
[10] T. Carell, J. Butenandt, *Angew. Chem.* **1997**, *109*, 1590−1593.
[11] G. Strukul, *Angew. Chem.* **1998**, *110*, 1256−1267.
[12] G. G. Melikyan, *Aldrichim. Acta* **1998**, *31*, 50−64.
[13] M. Shibasaki, H. Sasai, T. Arai, *Angew. Chem.* **1997**, *109*, 1290−1310.
[14] A. Blasko, T. C. Bruice, *Acc. Chem. Res.* **1999**, *32*, 475−484.
[15] N. H. Williams, B. Takasaki, M. Wall, J. Chin, *Acc. Chem. Res.* **1999**, *32*, 485−493.
[16] J.-M. Lehn, *Chem. Eur. J.* **1999**, *5*, 2455−2463.
[17] B. Jandeleit, D. J. Schaefer, T. S. Powers, H. W. Turner, W. H. Weinberg, *Angew. Chem.* **1999**, *111*, 2648−2689.
[18] D. E. Reichert, J. S. Lewis, C. J. Anderson, *Coord. Chem. Rev.* **1999**, *184*, 3−66.
[19] W.-W. V. Yam, K.-W. K. Lo, *Coord. Chem. Rev.* **1999**, *184*, 157−240.
[20] Z. Guo, P. J. Sadler, *Angew. Chem.* **1999**, *111*, 1610−1630.
[21] F. Ruan, Y. Chen, P. B. Hopkins, *J. Am. Chem. Soc.* **1990**, *112*, 9403.
[22] F. Ruan, Y. Chen, K. Itoh, T. Sasaki, P. B. Hopkins, *J. Org. Chem.* **1991**, *56*, 4347.
[23] K. Shah, T. M. Rana, *Synth. Commun.* **1996**, *26*, 2695−2702.
[24] B. Imperiali, S. L. Fisher, *J. Am. Chem. Soc.* **1991**, *113*, 8527−8528.
[25] B. Cuenod, A. Schepartz, *Tetrahedron Lett.* **1991**, *33*, 3325.
[26] B. Cuenod, A. Schepartz, *Science* **1993**, *259*, 510.
[27] R. Alsfasser, R. van Eldik, *Inorg. Chem.* **1996**, *35*, 628−636.
[28] B. Geißer, R. Alsfasser, *Eur. J. Inorg. Chem.* **1998**, 957−963.
[29] B. Geißer, A. Ponce, R. Alsfasser, *Inorg. Chem.* **1999**, *38*, 2030−2037.
[30] D. D. Cox, S. J. Benkovic, L. M. Bloom, F. C. Bradley, M. J. Nelson, L. Que, D. E. Wallick, *J. Am. Chem. Soc.* **1988**, *110*, 2026−2032.
[31] M. Bodanszky, A. Bodanszky, *The Practice of Peptide Synthesis*, Springer Verlag, Berlin, **1994**.
[32] D. Parker, *Chem. Soc. Rev.* **1990**, *19*, 271−291.
[33] A. A. Watson, A. C. Willis, D. P. Fairlie, *Inorg. Chem.* **1997**, *36*, 752−753.
[34] P. M. Angus, A. J. Elliot, A. M. Sargeson, A. C. Willis, *J. Chem. Soc., Dalton Trans.* **1999**, 1131−1136.
[35] C. S. Allen, C.-L. Chuang, M. Cornebise, J. W. Canary, *Inorg. Chim. Acta* **1995**, *239*, 29−37.
[36] A. Abufarag, H. Vahrenkamp, *Inorg. Chem.* **1995**, *34*, 2207−2216.
[37] J. Wirbser, H. Vahrenkamp, *Z. Naturforsch.* **1992**, *47b*, 962−968.
[38] J. Glerup, P. A. Goodson, D. J. Hodgson, K. Michelsen, K. M. Nielsen, H. Weihe, *Inorg. Chem.* **1992**, *31*, 4611−4616.
[39] J. W. Canary, C. S. Allen, J. M. Castagnetto, Y. Wang, *J. Am. Chem. Soc.* **1995**, *117*, 8484−8485.
[40] J. W. Canary, C. S. Allen, J. M. Castagnetto, Y.-H. Chiu, P. J. Toscano, Y. Wang, *Inorg. Chem.* **1998**, *37*, 6255−6262.
[41] G. Snatzke, *Angew. Chem.* **1968**, *80*, 15−26.
[42] L. Velluz, M. Legrand, *Angew. Chem.* **1965**, *77*, 842−850.
[43] P. Xie, M. Diem, *J. Am. Chem. Soc.* **1995**, *117*, 429−437.
[44] M. T. Werth, S.-F. Tang, G. Formicka, M. Zeppezauer, M. K. Johnson, *Inorg. Chem.* **1995**, *34*, 218−228.
[45] D. R. Benson, B. R. Hart, X. Zhu, M. B. Doughty, *J. Am. Chem. Soc.* **1995**, *117*, 8502−8510.
[46] M. Y. Ogawa, A. B. Gretchikhine, S. D. Soni, S. M. Davis, *Inorg. Chem.* **1995**, *34*, 6423.
[47] R. P. Bonomo, S. Pedotti, G. Vecchio, E. Rizzarelli, *Inorg. Chem.* **1996**, *35*, 6873−6877.
[48] R. P. Houser, M. P. Fitzsimons, J. K. Barton, *Inorg. Chem.* **1999**, *38*, 1368−1370.
[49] R. E. Austin, R. A. Maplestone, A. M. Sefler, K. Liu, W. N. Hruzewicz, C. W. Liu, H. S. Cho, D. E. Wemmer, P. A. Bartlett, *J. Am. Chem. Soc.* **1997**, *119*, 6461−6472.
[50] L. Grondahl, N. Sokolenko, G. Abbenate, D. P. Fairlie, G. R. Hanson, L. R. Gahan, *J. Chem. Soc., Dalton Trans.* **1999**, 1227−1234.
[51] R. Winter, F. Noll, *Methoden der Biophysikalischen Chemie*, Teubner, Stuttgart, **1998**.
[52] F. Hojland, H. Toftlund, S. Yde-Andersen, *Acta Chem. Scand.* **1983**, *A37*, 251−257.
[53] J. K. Romary, R. D. Zachariasen, J. D. Barger, H. Schiesser, *J. Chem. Soc. C* **1968**, 2884.
[54] Siemens Area Detector Absorption Correction, Siemens.
[55] G. M. Sheldrick, *SHELX-97*; Universität Göttingen, **1997**.
[56] L. Zsolnai, *xpma, zortep*, Universität Heidelberg, **1997**.

Received December 2, 1999
[I99439]